

## Accelerated Publications

---

### Global Disruption of the WASP Autoinhibited Structure on Cdc42 Binding. Ligand Displacement as a Novel Method for Monitoring Amide Hydrogen Exchange<sup>†</sup>

Matthias Buck, Wei Xu, and Michael K. Rosen\*

Howard Hughes Medical Institute, Cellular Biochemistry and Biophysics Program, Memorial Sloan-Kettering Cancer Center,  
1275 York Avenue, New York, New York 10021

Received August 24, 2001; Revised Manuscript Received October 1, 2001

**ABSTRACT:** The Cdc42 GTPase, a member of the Rho subfamily of Ras proteins, can signal to the cytoskeleton through its effector, the Wiskott-Aldrich syndrome protein (WASP), activation of which results in localized polymerization of new actin filaments. NMR structures of WASP peptide models in the Cdc42-bound and free states suggest that GTPase binding weakens autoinhibitory contacts between the GTPase binding domain (GBD) and the C-terminal actin regulatory (VCA) region of the protein. In the study presented here, amide hydrogen exchange has been used with NMR spectroscopy to directly examine destabilization of the autoinhibited GBD–VCA conformation caused by GTPase binding. A truncated protein, GBD-C, which models autoinhibited WASP, folds into a highly stable conformation with amide exchange protection factors of up to  $3 \times 10^6$ . A novel hydrogen exchange labeling-quench strategy, employing a high-affinity ligand to displace Cdc42 from WASP, was used to examine the amide exchange from the Cdc42-bound state of GBD-C. The GTPase increases exchange rates of the most protected amides by 50–500-fold, with destabilization reducing the differences in the protection of segments in the free state. The results confirm that Cdc42 facilitates the physical separation of the GBD from the VCA in a tethered molecule, indicating this process likely plays an important role in activation of full-length WASP by the GTPase. However, destabilization of GBD-C is not complete in the Cdc42 complex. The data indicate that partitioning of free energy between binding and activation may limit the extent to which GTPases can cause conformational change in effectors. This notion is consistent with the requirement of multiple input signals in order to achieve maximal activation in many effector molecules.

GTPases in the Ras superfamily function as molecular switches in diverse systems, controlling processes such as cytoskeletal change, cell growth and vesicle transport. The GTPases cycle between an inactive GDP-bound state and an active GTP-bound state *in vivo*. In the GTP<sup>1</sup> state, they

are capable of binding to and activating downstream effector proteins. In recent years, multiple effectors have been discovered for many members of the superfamily. It is

<sup>†</sup> M.K.R. is an investigator of the Howard Hughes Medical Institute and gratefully acknowledges additional support from the National Institutes of Health (Grant GM56322). M.B. is the recipient of an NIH postdoctoral fellowship (GM20502).

\* To whom correspondence should be addressed. Phone: (212) 639-8724. Fax: (212) 717-3135. E-mail: rosen@mrnmr1.mskcc.org.

<sup>1</sup> Abbreviations: CRIB, Cdc42/Rac interactive binding; DMSO, dimethyl sulfoxide; DTT, dithiothreitol; GBD, GTPase binding domain; GDP, guanosine 5'-diphosphate; GMPPNP,  $\beta,\gamma$ -imidoguanosine 5'-triphosphate; GTP, guanosine 5'-triphosphate; HSQC, heteronuclear single quantum coherence; NMR, nuclear magnetic resonance; PAK, p21-activated kinase; PIP<sub>2</sub>, phosphatidylinositol 4,5-bisphosphate; VCA, verprolin-cofilin homology and acidic region of WASP; WASP, Wiskott-Aldrich syndrome protein.

generally believed that the subset of these molecular targets, utilized in response to a particular stimulus, determines the resultant specific cellular response. But the structural and biophysical factors that determine the engagement of a particular effector and the means by which interaction is coupled to activation are poorly understood (1).

Ras homologues in the Rho subfamily, including Cdc42, Rac, and Rho, play important roles in signaling pathways that control cell morphology, adhesion, motility, and gene expression (2). Cdc42 appears to function often as a regulator of cell polarity, frequently through inducing localized polymerization of new actin filaments (3). Many Cdc42-dependent processes are mediated through downstream effectors containing a conserved, 12–16-residue sequence termed a CRIB (for Cdc42/Rac Interactive Binding) motif that has now been identified in more than 25 different proteins (4). Biochemical and structural studies of several effector protein–Cdc42 interactions have revealed a conserved mode of interaction between the GTPase and CRIB motif, involving extension of the GTPase  $\beta$ -sheet with an additional strand (5–7). In all cases examined to date, additional effector-specific regions located immediately adjacent to the CRIB motif are involved in intramolecular interactions which play an important role in autoinhibition of the free effectors (8, 9). Disruption of these interactions by GTPase binding is critical for activation.

The Wiskott-Aldrich syndrome protein (WASP) is a CRIB motif-containing Cdc42 effector and a critical component of pathways that link extracellular signals to the actin cytoskeleton (10–12). WASP stimulates cytoskeletal rearrangement through binding and activation of Arp2/3 complex, an important actin nucleating and cross-linking factor in the cell (13). The ability of WASP to stimulate Arp2/3 complex is controlled by an autoinhibitory mechanism, characterized by intramolecular interactions in WASP between the central GTPase binding domain (GBD, containing the CRIB motif and adjacent sequences) and the C-terminal VCA region (weakly homologous to verprolin, cofilin, and an acidic C-terminus) (8, 14, 15). These interactions block the ability of the VCA region to stimulate Arp2/3 complex, although the exact mechanism of autoinhibition remains unclear and may involve a series of basic residues immediately N-terminal to the CRIB motif (16). Binding of Cdc42 has been shown to physically displace GBD peptides from VCA peptides, concomitant with enabling the VCA to activate Arp2/3 complex. It is therefore likely that separation of these regions of the polypeptide chain, facilitated by Cdc42-induced destabilization of the GBD–VCA conformation, is integral to the mechanism by which WASP is activated by the GTPase. A molecular mechanism of this destabilization was suggested by comparison of the structures of a GBD–Cdc42 complex and a model for the GBD–VCA complex. The two structures were found to be incompatible with one another, indicating that binding of Cdc42 to the GBD could disrupt many contacts in the autoinhibited conformation. A similar mechanism, involving destabilization of an autoinhibited structure on binding to Cdc42, has been proposed for the activation of p21-activated kinase (PAK) (9), another CRIB motif-containing effector. However, the regions of the structure that are affected by Cdc42 binding and the magnitude of their destabilization have not been determined. In the study presented here, we use amide

hydrogen exchange, which is a sensitive probe for the stability of protein main chain structure, to examine these issues.

The rates of amide proton exchange with solvent provide important information about protein dynamics, folding, and stability (17–19). In a typical experiment, a protein sample is prepared to the desired state (e.g., native, ligand-bound, or a substantially unfolded conformation) and then a rapid change of conditions allows “labeling” of protein amide sites, for example, by hydrogen exchange with solvent deuterons. After a defined period of time, hydrogen exchange is “quenched” by a second rapid change into conditions where further exchange is ideally eliminated (e.g., low pH or denaturant concentration) and the amide hydrogen–deuterium population of the protein can be readily measured. At present, experiments based on amide hydrogen exchange employ one or a combination of quenching conditions. A) the pH is adjusted to near 4, where exchange is minimal for main chain amides (20). B) the temperature is lowered to minimize exchange. C) the solvent is replaced nearly completely with an aprotic medium such as DMSO (21) or a structure-stabilizing cosolvent, such as trimethylamine *N*-oxide (22) or trifluoroethanol (M. Buck et al., manuscript in preparation), is added. D) the denaturant or ligand is removed from the sample by dilution followed by rapid filtration or chromatography, returning the protein to a state that protects amides well (23).

In this report, we describe a novel method for quenching amide exchange from the Cdc42-bound state of WASP. The procedure must both dissociate the Cdc42–WASP complex and allow WASP to revert to the state of the free protein. We find that addition of a ligand that binds Cdc42 more tightly than WASP displaces the latter and allows it to regain the structure of the autoinhibited state, where many amides are highly protected from hydrogen exchange. We call this strategy “ligand displacement”; it is formally akin to procedure D above except that the ligand is displaced rather than removed from the solution. The general utility of the ligand displacement strategy as a quench in hydrogen exchange experiments is discussed below.

Hydrogen exchange measurements allow us to quantify the effects of GTPase binding on the stability of different segments of the WASP model protein. The data indicate a large global destabilization of the WASP autoinhibited conformation on interaction with Cdc42, consistent with the structural incompatibility of the two states (8). Interestingly, in the construct used here, which is more highly stabilized than native WASP, this energy is not sufficient to fully unfold the protein, and significant protection against amide hydrogen exchange (100–3000-fold) remains in the bound state. Features of Cdc42–effector interactions are reviewed in light of our findings, and parallels are drawn to other systems.

## MATERIALS AND METHODS

**Constructs and Proteins.** Preparation and purification of Cdc42 loaded with a nonhydrolyzable analogue of GTP (GMPPNP) and WASP fragments have been described elsewhere (5, 8). The WASP fragment of residues 225–310 linked to residues 461–492 with a (GGG)<sub>2</sub> linker (denoted GBD-C) used in this study was labeled with <sup>15</sup>N and purified in a similar manner.

**Experimental Procedure for Hydrogen Exchange.** The GBD-C protein was lyophilized from 250  $\mu$ L of 50 mM phosphate buffer (pH 6.3), 100 mM NaCl, 5 mM MgCl<sub>2</sub>, and 5 mM DTT, and redissolved in the same volume of 99.9% D<sub>2</sub>O to 0.3 mM by rapid pipetting. For analyses of bound GBD-C, 250  $\mu$ L of a 0.45 mM Cdc42-GMPPNP solution (phosphate buffer as above in a 10% H<sub>2</sub>O/90% D<sub>2</sub>O mixture) was added immediately and mixed. The reaction was quenched after 1, 5, 10, 20, 40, 80, and 160 min at 15 °C, by addition of 250  $\mu$ L of a 30% H<sub>2</sub>O/70% D<sub>2</sub>O solution of the GBD (0.9 mM), followed by concentration to 250  $\mu$ L using ultrafiltration (55 min at 4 °C). The pD values of the exchange samples were found to be within 0.05 unit of 6.3 (electrode reading uncorrected for isotope effects).

**NMR Data Acquisition and Analysis.** Each sensitivity-enhanced <sup>1</sup>H–<sup>15</sup>N HSQC spectrum (44) was recorded in 60 min at 15 °C on a Varian Inova 600 spectrometer. Peak volumes were integrated and compared to baseline noise for error estimation (4% uncertainty in the first time point). In analyses of the GBD-C–Cdc42 complex, to correct for variations in sample concentration during workup, peak volumes were scaled to the average peak volume of residues 256, 480, 483, 491, and 492 which are not protected from exchange in GBD-C and report the 13% level of residual H<sub>2</sub>O in the final sample. Scaled amide intensities in a sample at 0.1 mM were nearly identical to those in the higher-concentration samples, excluding the possibility that hydrogen exchange is slowed due to aggregation. A single exponential ( $y = a \exp -kt + \text{residual water offset}$ ) was used to fit the peak volume data and to determine the exchange rate,  $k$ . To assess exchange during sample preparation and spectral acquisition, spectra were acquired on a sample prepared by simultaneously adding the GBD and Cdc42 to <sup>15</sup>N-labeled GBD-C but which was otherwise treated in a manner identical to that of the samples of the labeling exchange time course, thus providing a zero time point as a control. For amides with partial exchange during the sample preparation and NMR data acquisition, the intensity that remains in this time zero control was compared that expected to remain using the relationship  $y = (1 - \text{offset}) \exp -k'(\text{NMR acquisition} + \text{sample preparation time}) + \text{offset}$  (here 0.13) as an estimate, where  $k'$  is the rate of exchange from free GBD-C and assuming the intensity buildup in spectra is dominated by the first third of the acquisition time. The hydrogen exchange rate during preparation is corrected for temperature. We similarly compared the intensity change in two consecutively recorded 1 h <sup>1</sup>H–<sup>15</sup>N HSQC spectra of this control sample and also compared with intensities of a spectrum recorded in a 90% H<sub>2</sub>O/10% D<sub>2</sub>O mixture, as a sample not affected by exchange. A group of 12 amides which have exchange rates faster than 0.75 h<sup>–1</sup> were excluded from the analysis. Intrinsic exchange rates were calculated with residue specific correction factors (20) and were corrected for temperature.

## RESULTS AND DISCUSSION

**Development of a Hydrogen Exchange Strategy for Studying Cdc42-Bound WASP.** We have used hydrogen exchange and NMR spectroscopy to examine how binding of Cdc42 alters the stability and dynamics of an effector protein, WASP. We and others have developed model proteins of WASP in which the GBD region is joined to portions of the

VCA through a short linker, rather than through the large proline-rich segment found in the wild-type molecule. The protein used here, GBD-C, links residues 225–310 to residues 461–492 with a (GGG)<sub>2</sub> linker and, isolated from other binding partners, adopts a folded structure we refer to as the autoinhibited state (8). Such models are biochemically more tractable than full-length WASP, while retaining many of the essential features. However, the shorter linker significantly stabilizes the autoinhibited conformation in these systems relative to the wild type. Thus, some aspects of function may differ quantitatively from those of WASP, and the data must be considered with this in mind.

NMR spectra of Cdc42-bound GBD-C have extremely broad lines (not shown), preventing direct analysis of this state of the protein. Therefore, we developed a procedure that allows amide exchange to be monitored from the Cdc42 complex through analysis of spectra of free GBD-C, where resonances are narrow and easily quantifiable. The method involves a quenching step, which we call ligand displacement. The experimental protocol, pictured in Figure 1, makes use of a WASP fragment (GBD, residues 230–288) that binds Cdc42 with a  $K_d$  of 11 nM, an affinity approximately 340-fold tighter than that of the autoinhibited GBD-C construct whose dynamic behavior we want to study ( $K_d = 3.5 \mu$ M). In the procedure, [<sup>15</sup>N]GBD-C is exposed to unlabeled Cdc42 for a defined labeling period. An excess of unlabeled GBD peptide is then added, which displaces [<sup>15</sup>N]GBD-C from the GTPase, allowing it to revert to the autoinhibited conformation. As the free state highly protects many amides, displacement effectively quenches hydrogen exchange. Since the unlabeled GBD and Cdc42 are not featured in the NMR spectra of the <sup>15</sup>N-labeled GBD-C, spectra may be recorded without separation of the components. The effectiveness of this method requires several conditions. First, hydrogen exchange from free GBD-C must be much slower than the sample preparation and NMR acquisition times. Second, displacement of GBD-C from Cdc42 in the quench must be complete, and allow the protein to regain the structure of the autoinhibited state. Finally, displacement and the conformational change must be rapid with respect to the rate of hydrogen exchange from the complex. The following section reports on controls for ascertaining each of these requirements.

Hydrogen exchange was measured in a sample of WASP GBD-C at 15 °C in D<sub>2</sub>O buffer (pH 6.3), allowing us to derive protection factors for 38 amides. These range from  $1.6 \times 10^2$  to  $2.6 \times 10^6$  (summarized in Table 1). Protection factors were greatest in the center of the  $\alpha$ -helices, with an average value of  $6 \times 10^4$ . Hydrogen exchange was sufficiently rapid in the  $\beta$ -strands that we could not measure protection factors for any amides in these elements. For 16 of the 38 amides, exchange rates were relatively rapid, ranging from  $3.0 \times 10^{-2}$  to  $6 \times 10^{-3} \text{ min}^{-1}$ . Although these amides could be observed in spectra of freshly dissolved GBD-C, the sample handling period following the quench (~55 min) is sufficiently long in the ligand displacement experiments that all but four of these amides have largely exchanged and their peak volumes cannot be accurately measured. The four slower exchanging amides of this group have rates in the quenched mixture that are similar compared to those obtained for the protein in isolation (see Materials and Methods), suggesting that the quench of their exchange



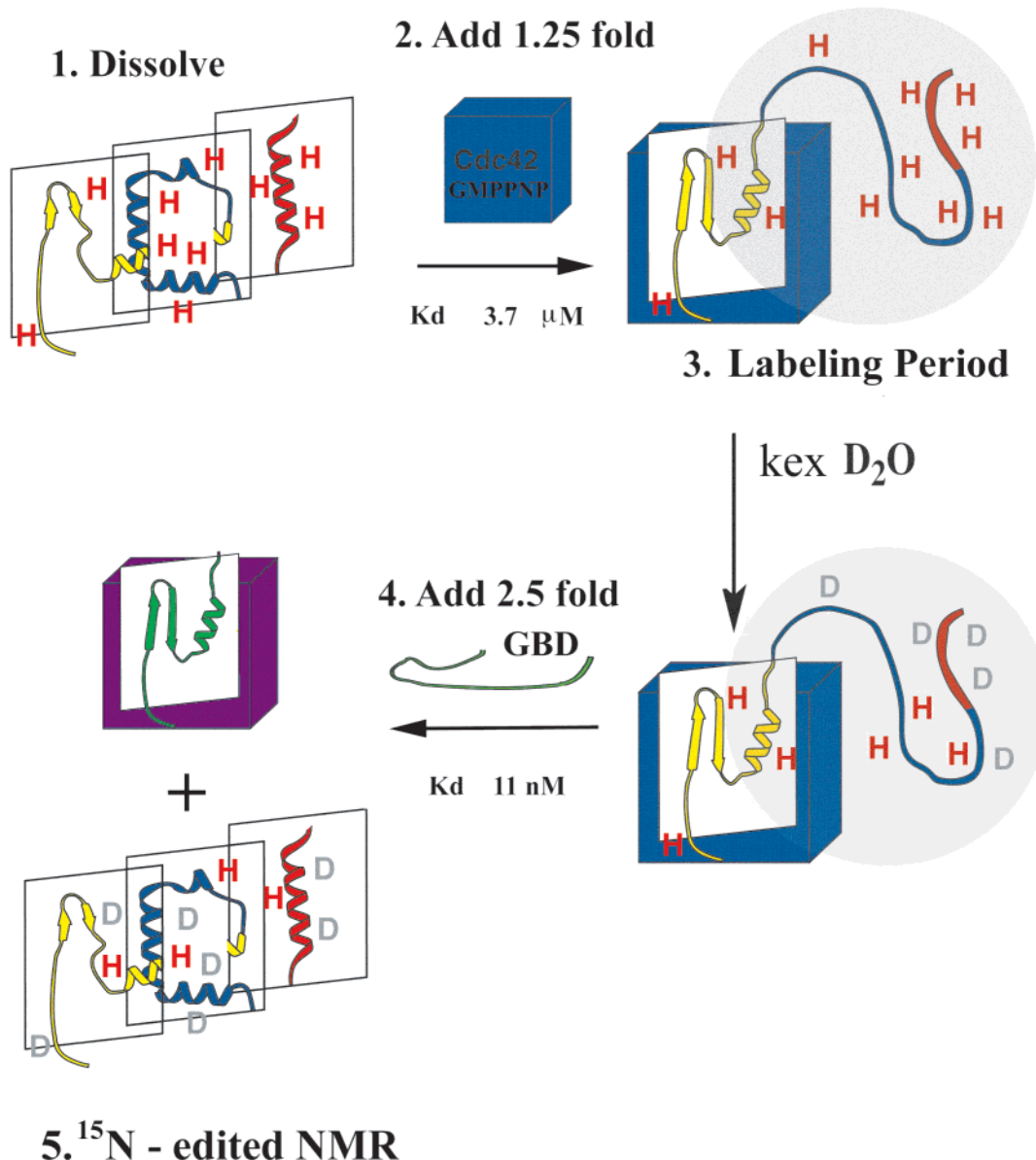


FIGURE 1: Pulse quench strategy using ligand displacement. (1) WASP GBD-C is dissolved in  $\text{D}_2\text{O}$ . In isolation, the protein exists in an autoinhibited conformation which highly protects many of the amides. (2) A 1.25-fold excess of Cdc42 is added, destabilizing autoinhibited WASP and initiating hydrogen exchange. The concentrations and  $K_d$  ( $3.7 \mu\text{M}$ ) indicate that approximately 96% of the GBD-C WASP molecules are bound by the GTPase. (3) Hydrogen exchange proceeds during the labeling period of duration  $t$ . The structure of the protein bound to Cdc42 (shaded gray) is unknown but allows greater access to amide exchange than the autoinhibited conformation. (4) At the end of the labeling period, a 2.5-fold excess of the GBD peptide, which binds Cdc42 approximately 340-fold more tightly than GBD-C WASP, is added, displacing the GBD-C and allowing it to revert to its autoinhibited conformation. Displacement quenches hydrogen exchange to  $>99.7\%$  (0.3% of the GBD-C-Cdc42 complex remains), highly protecting 26 of the 121 main chain amides. (5) The sample is prepared for NMR, and a  $^1\text{H}$ - $^{15}\text{N}$  HSQC spectrum is recorded, enabling selective observation of GBD-C in the presence of unlabeled Cdc42 and GBD peptide.

is effective. The other 22 amides have exchange rates slower than  $3.0 \times 10^{-3} \text{ min}^{-1}$  in the free protein and exhibited no significant exchange ( $<10\%$  change in amide occupancy) in the quenched mixture during sample preparation or spectral acquisition (see Materials and Methods). Thus, for 26 amides in GBD-C, hydrogen exchange is sufficiently slow following the quench that it can be quantitatively accounted for or neglected.

The WASP state is substantially destabilized on Cdc42 binding, as inferred from the spectra of the complex (M. Buck and M. K. Rosen, manuscript in preparation), and consequently, we anticipated that exchange of amide hydrogens from the complex would be faster by several orders of

magnitude. Representative regions of  $^1\text{H}$ - $^{15}\text{N}$  HSQC spectra recorded with different labeling times are shown in Figure 2a. Several features are notable. After the quench, GBD-C chemical shifts and line widths are nearly identical to those of the free protein alone in solution, indicating that the protein has reverted to the autoinhibited conformation and that the population of Cdc42-bound GBD-C is small. Less than 0.3% of GBD-C is expected to be complexed on the basis of the binding constants of WASP GBD-C ( $K_d = 3.7 \mu\text{M}$ ) and the GBD peptide ( $K_d = 11 \text{ nM}$ ). A small population of bound WASP would have a negligible effect on amide intensities on the time scale needed for data acquisition (M. Buck and M. K. Rosen, manuscript in preparation).

Table 1: Summary of Amide Exchange Data<sup>a</sup>

residues	$k_{\text{int}}$ (min <sup>-1</sup> )	log $P$ bound	log $P$ free	difference
$\alpha$ 1 (267, 268, 270–272, 274)	25.5	$2.42 \pm 0.28$	$4.51 \pm 0.74$	$2.12 \pm 0.77$
$\alpha$ 2 (281)	22.4	$2.27 \pm 0.09^b$	$4.27 \pm 0.04^b$	$2.00 \pm 0.13^b$
$\alpha$ 3 (289–295)	10.5	$2.71 \pm 0.52$	$5.48 \pm 0.79$	$2.69 \pm 0.58$
$\alpha$ 4 (303, 304)	19.7	$2.62 \pm 0.37$	$3.93 \pm 0.80$	$1.73 \pm 0.30$
$\alpha$ 5 (470, 471, 473, 474)	45.8	$2.45 \pm 0.40$	$4.24 \pm 0.96$	$1.79 \pm 0.75$
average	$23.3 \pm 30.8$	$2.56 \pm 0.41$	$4.77 \pm 0.89$	$2.21 \pm 0.71$

<sup>a</sup> Column 1: residues belonging to secondary structural elements used for averaging. Column 2: average intrinsic exchange rate ( $k_{\text{int}}$ ). Column 3: average of log protection factor ( $P$ ) of those amides in the Cdc42-bound state. Column 4: average of log protection factors in the unbound, autoinhibited protein. Column 5: average of the difference between log protection factors. The errors ( $\pm$ ) are one standard deviation of the values averaged. <sup>b</sup> Data for one residue; the error is the uncertainty in fitting the exchange rate. The last row gives the average over all residues listed.

Rapid displacement of the GBD-C protein from Cdc42 is a further requirement for the labeling-quench protocol to be successful in these experiments. If binding and displacement kinetics were slow, amide intensity changes would reflect both the exchange from the Cdc42-bound state and the kinetics of the conformational changes on binding and dissociation, in principle yielding multiexponential decays. Multiexponentials are not required to fit the amide intensity decay data. Moreover, during measurement of Cdc42–WASP affinities using fluorescence spectroscopy and isothermal scanning calorimetry, we (M. K. Rosen and A. S. Kim, unpublished observation; 8) and others (24) have qualitatively observed that binding of a variety of WASP constructs to the GTPase is complete within 1–2 s for protein concentrations in the range of 0.5–10  $\mu$ M. Dissociation rates are similarly rapid, and we have seen that a fluorophore-tagged GBD-C protein can be displaced by the GBD in less than 5 s with concentration ratios similar to that used in the hydrogen exchange experiments (data not shown). Once displaced, the GBD-C should assume the stable autoinhibited state on a time scale that is much faster than the shortest labeling period (1 min), given that conformational changes, such as folding processes, are fast (usually in the 10–100 ms range for typical monomeric proteins).

We have shown in the section above that it is possible to use a competitive, high-affinity ligand (GBD) to displace a low-affinity ligand of interest (GBD-C) from a protein binding partner (Cdc42). The conformation of the displaced ligand reverts to a state allowing no further exchange of amides so that the amide hydrogen occupancy reports on exchange that occurred while in the bound state. Therefore, the exponential decrease in amide intensity as a function of labeling period represents exchange from the Cdc42-bound state. Representative data in Figure 2b show that exchange in GBD-C is much faster in the complex state than in the free protein.

*Comparison of the Ligand Displacement Strategy with Other Techniques, and Its General Utility.* When protein complexes are not amenable to NMR analysis, components must be separated in order to perform hydrogen exchange studies. In existing strategies, this often takes the form of physical (e.g., chromatographic) separation of the components, as in reported studies of protein–antibody complexes (25, 26) and amyloid fibrils (27, 28). However, such

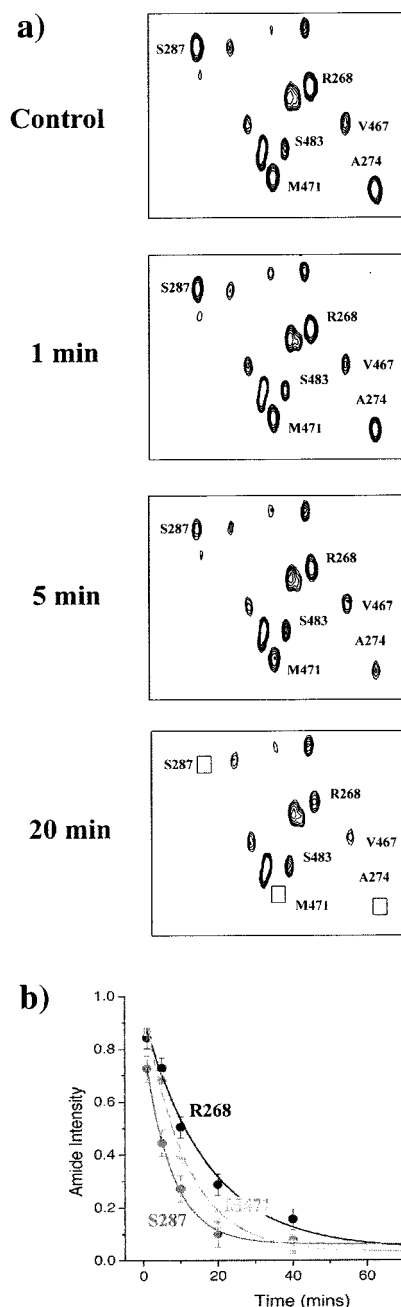


FIGURE 2: (a) Amide exchange data illustrated for a representative region of the <sup>1</sup>H–<sup>15</sup>N HSQC spectra. Spectra for the control, with Cdc42 and the GBD added simultaneously, and exchange quenched after 1, 5, and 20 min are shown. Amides S287, R268, A274, V467, and M471 have similar intensities in a control sample (immediate quench of exchange) but have different intensities in spectra of the protein that had been bound to Cdc42, reporting on different rates of exchange while in the Cdc42-bound state. S483 is one of the five residues used for the internal scaling of the protein concentration. (b) Time course showing the intensity decrease in samples quenched at the different times and fits to exponential decays.

procedures typically require significant perturbation of solution conditions, and cannot be used with many systems. The principal advantage of the ligand displacement strategy is that a molecule of interest can be dissociated from a complex without physical separation of all the components, and thus without significant perturbation of conditions. In principle, the competitor and protein under investigation need not be related. For example, it should be possible to probe other Cdc42–effector interactions (Pak, Ack, etc.) using the WASP

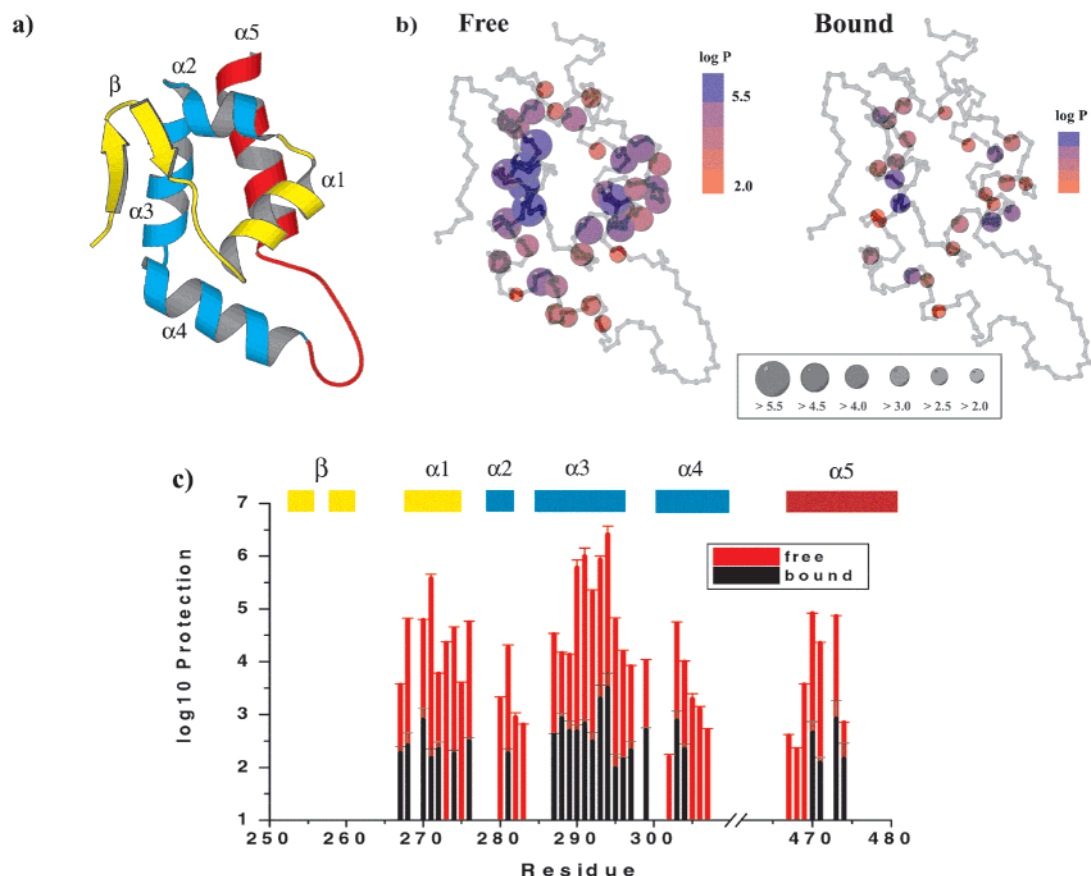


FIGURE 3: (a) Schematic representation of the autoinhibited conformation of WASP. The structured parts of the GBD (residues 250–276) and the cofilin homology helix (residues 461–479) regions are shaded yellow and red, respectively. (b) Location and magnitude of protection factors in the free and Cdc42-bound state as indicated on the backbone of the autoinhibited structure. The scaled range of the data is indicated by color (red to blue via purple), whereas the absolute value is indicated by the size of the spheres. (c) Log of protection factors of amides in free (red) and Cdc42-bound WASP (black) as a function of protein sequence. The secondary structure determined by NMR in the native, unbound protein is also shown. For the 15 amides that could be monitored in free GBD-C, but exchanged too rapidly in the complex, only a red bar is shown. The sites that exchange too quickly to be followed in the free protein, such as those belonging to the  $\beta$ -hairpin and a helical turn of the GBD (residues 252–263), could, in principle, be more highly protected in the complex.

GBD peptide, as long as the GBD is the ligand with a higher affinity for the GTPase. The ligand displacement procedure need not result in a free protein but instead could involve ligand substitution. Indeed, experiments are in progress in our laboratory that use unlabeled GBD and GBD-C to monitor hydrogen exchange from  $[^{15}\text{N}]\text{Cdc42}$  in the two complexes. Furthermore, even if ligand substitution does not cause a large difference in hydrogen exchange rates, it could still be useful in cases where the dynamics or the chemical stability of the original ligand is unfavorable for NMR spectroscopic analysis. As long as hydrogen exchange is slow enough from the reference state to allow NMR detection, such experiments will reveal the difference in hydrogen exchange of the components involved. The strategy may thus be generalizable to cases in which the stability and dynamics of several protein binding partners are of interest. The use of ligand substitution may open a door to new investigations of protein functional dynamics using amide hydrogen exchange.

**Destabilization of Cdc42-Bound GBD-C Measured by Hydrogen Exchange.** In the structure of GBD-C, a model for autoinhibited WASP that has been determined by NMR spectroscopy (8), the GBD, and part of the VCA interact to form a small, cooperatively folded domain, which can be considered as three layers of secondary structural elements in Figure 3a ( $\beta$ -hairpin and  $\alpha 1$  helix, helices  $\alpha 2$ – $\alpha 4$ , and

helix  $\alpha 5$ ). Layers 1 and 2 compose the GBD, and layer 3 is the “cofilin homology” region of the VCA. The first layer is known to bind Cdc42 in a conformation that is incompatible with the remainder of the autoinhibited structure. Thus, binding is likely to destabilize at least part of the GBD-C structure (5, 8). We tested this model by examining hydrogen exchange rates of GBD-C in complex with Cdc42. Using the methodology described above, we could fit amide hydrogen intensities for 26 residues throughout the WASP structure as a function of the time that allowed hydrogen exchange to occur from the Cdc42-bound state. Protection factors, which compare the exchange rates to those calculated for residues in a random coil conformation, can provide information about the stability of the structures that are responsible for the retardation of exchange. These are shown as a function of the GBD-C sequence in Figure 3c, along with secondary structural elements, and thus provide site specific probes for the effect of Cdc42 binding. The amide protection factors, also summarized in Table 1, demonstrate that binding to Cdc42 has considerably increased rates of exchange across the autoinhibited conformation. The exchange rates are increased in WASP GBD-C by a factor of 130 on average compared to those of the same residues in the unbound protein. This effect could, in principle reflect an increase in only local fluctuations of the protein, without an overall thermodynamic destabilization. However, we think

this is unlikely since we have shown elsewhere (M. Buck and M. K. Rosen, manuscript in preparation) that exchange occurs in the EX2 regime and since the increase in exchange rates is seen across the entire structure. It also includes the most highly protected amides, which are likely to exchange by fluctuations approaching global unfolding. Thus, the pattern of deprotection indicates a global destabilization of the autoinhibited conformation. Some variations in the level of destabilization exist for different elements of secondary structure. The  $\alpha 3$  helix, which forms a significant part of the hydrophobic core of the autoinhibited structure, is destabilized most ( $\sim 500$ -fold change in rates), while helices  $\alpha 4$  and  $\alpha 5$ , which are furthest in sequence from the Cdc42 binding site, are affected least ( $\sim 50$ – $60$ -fold). Although helix  $\alpha 5$  is not sequence adjacent but linked to the GBD structure, its destabilization is still similar to that of the GBD structure. Interestingly, the secondary structural elements with greater stability in GBD-C exhibit greater destabilization (larger increases in hydrogen exchange rates) on binding to Cdc42 (see Table 1). Thus, binding serves to bring protection against hydrogen exchange across the molecule to a more similar level.

The protection factors in Cdc42-bound WASP GBD-C range from  $10^2$  to  $10^3$ . If we assume a two-state model involving only bound and unbound species, this would imply that the bound protein is maintained in a partially ordered conformation in which the helices have considerable persistency (23, 29). Alternatively, several Cdc42-bound states may account for the protection factors. In this case, a small population of relatively unstructured protein could be sufficient to cause the observed amide exchange kinetics. We have confirmed the magnitude of the protection factors in the Cdc42-bound state of GBD-C by a separate set of experiments, which use the GTPase at much lower, hydrogen exchange catalytic concentrations (e.g., 0.025 molar equiv to WASP) but under otherwise similar solution conditions. These data are consistent with the results shown here and will be reported elsewhere, together with a discussion of the different models for hydrogen exchange from the Cdc42-bound state (M. Buck and M. K. Rosen, manuscript in preparation).

It is of interest to note here that the pattern of amides which are most highly protected in the Cdc42-bound state of GBD-C coincides qualitatively with the locations of amides whose rate is most strongly retarded in the unbound state (e.g., F292 and I293 at the C-terminal side of helix  $\alpha 3$ , V303 and R304 in helix  $\alpha 4$ , and V473 in helix  $\alpha 5$ ). This suggests that some of the interactions that stabilize these helices in the Cdc42-bound state are similar to those in the autoinhibited state. An interesting exception is helix  $\alpha 1$ . Here the most protected amide is L270 in the Cdc42-bound state (with a protection factor of 780, approximately 3 times that of the surrounding residues), whereas F271 is the most protected residue in helix  $\alpha 1$  in the unbound state (protection factor of  $3.7 \times 10^5$ , almost 5 times higher than for the surrounding residues), suggesting that the interactions of this helix are altered in the Cdc42-bound state. Intriguingly, the helix  $\alpha 1$  is known to have direct interactions with Cdc42 in the Cdc42–GBD complex (5) and may be the primary site of the conformational change that occurs in WASP upon Cdc42 binding (M. K. Rosen and M. Buck, unpublished observation).

The data here support the notion that structural incompatibility leads to destabilization of the core of the autoinhibited domain on binding to Cdc42. The energy necessary for this disruption must be drawn from the GBD binding energy. This is consistent with the appreciably decreased affinity of GBD-C compared to that of the GBD alone [ $3.5 \mu\text{M}$  for GBD-C compared to  $10$ – $130 \text{ nM}$  for various GBD constructs (5, 8, 30)]. Similar data have been obtained for the p21 activated kinase (PAK), where the full-length protein interacts with Cdc42 with a 100-fold lower affinity than the minimal binding element (31). In other autoinhibited proteins, the effects of configurational entropy in the isolated activator-binding domain or of strain in the full-length protein could serve to equalize the affinities of the two polypeptides (32), and could in principle reverse them. However, it is likely that the exchange of binding energy for activation or conformational change will be a property of many autoinhibited systems.

We are presently investigating other WASP constructs to determine the relationship between binding affinity, WASP protein stability, and the extent of activation by GTPase. The results reported here indicate that Cdc42 is not able to completely destabilize structure in GBD-C. This suggests that it may not be possible to use all the energy that is available from binding Cdc42 to effect conformational change in autoinhibited effectors since this could, in principle, result in a very weakly bound complex. Incomplete disruption, and thus potentially incomplete activation, by a single signaling input could have important mechanistic consequences. For example, in the case of PAK, recently published data (31) indicate that Cdc42 binding may not be sufficient to completely disrupt the autoinhibited dimer or give complete activation. Rather, the GTPase provides limited destabilization of the autoinhibitory switch domain, which is sufficient to facilitate autophosphorylation. The covalent modification then appears to cause dissociation of the dimer, affording complete and GTPase-independent activation. Thus, limited activation by the GTPase allows PAK to function as a switch, activation of which is triggered by GTPase but the lifetime of which is independent of the rise and fall of the nucleotide cycle. The amount of destabilization energy that is required for a given system will be determined by the extent of the incompatibility between the free and bound structures and by the precise balance of interactions that are disrupted or created in the binding process. Thus, it may be different for different targets of the GTPase. In the context of WASP activation, incomplete destabilization of the autoinhibited state by Cdc42 may have a biological purpose. Recent evidence suggests that at low Cdc42 concentrations additional signaling inputs, such as PIP<sub>2</sub>, Grb2, Nck, or profilin, are required to effect WASP activation (15, 33–37). Thus, by setting the threshold for activation higher than a level that can be achieved by a single signal, a number of signaling inputs may be integrated, allowing both tighter control in binary switch mechanisms and a greater range of response, in case of proportional or cooperative systems.

The WASP–Cdc42 complex is one of relatively few characterized examples to date where macromolecular interactions lead to large-scale destabilization of a protein. However, other important examples have been reported. Binding of chaperones can lead to destabilization of certain



substrates (38, 39), which is likely to be critical in chaperone function of dissociating partially folded proteins prior to refolding them (38, 40). Serpins, such as  $\alpha$ -1 antitrypsin, cause extensive structural disruption in the protease trypsin, thus inhibiting the enzyme (41). Several cases have also emerged in which interaction with DNA destabilizes proteins (42). In the transcription factor Ets-1, for example, DNA binding unfolds and releases an inhibitory N-terminal helix of the protein, which is then available for binding to other proteins (43). The ability of proteins to undergo conformational transitions has been extensively exploited for regulatory and for signal transduction purposes in cells. The method described in this report adds to a wide repertoire of biophysical techniques that can be used to investigate mechanisms that involve changes in protein conformational stability on complex formation.

## REFERENCES

- Boguski, M., and McCormick, F. (1993) *Nature* 366, 643–654.
- Hall, A. (1998) *Science* 279, 509–514.
- Johnson, D. I. (1999) *Microbiol. Mol. Biol. Rev.* 63, 54–105.
- Burbelo, P. D., Drechsel, D., and Hall, A. (1995) *J. Biol. Chem.* 270, 29071–29074.
- Abdul-Manan, N., Aghazadeh, B., Liu, G. A., Majumdar, A., Ouerfelli, O., Siminovich, K. A., and Rosen, M. K. (1999) *Nature* 399, 379–383.
- Mott, H. R., Owen, D., Nietlispach, D., Lowe, P. N., Manser, E., Lim, L., and Laue, E. D. (1999) *Nature* 399, 384–388.
- Morreale, A., Venkatesan, M., Mott, H. R., Owen, D., Nietlispach, D., Lowe, P. N., and Laue, E. D. (2000) *Nat. Struct. Biol.* 7, 384–383.
- Kim, A. S., Kakalis, L. T., Abdul-Manan, N., Liu, G. A., and Rosen, M. K. (2000) *Nature* 404, 151–158.
- Lei, M., Lu, W., Meng, W., Parrini, M. C., Eck, M. J., Mayer, B. J., and Harrison, S. C. (2000) *Cell* 102, 387–397.
- Bi, E., and Zigmond, S. H. (1999) *Curr. Biol.* 9, R160–R163.
- Carlier, M.-F., Ducruix, A., and Pantaloni, D. (1999) *Chem. Biol.* 6, R235–R240.
- Machesky, L. M., and Insall, R. H. (1999) *J. Cell Biol.* 146, 267–272.
- Higgs, H. N., and Pollard, T. D. (2001) *Annu. Rev. Biochem.* 70, 649–676.
- Miki, H., Sasaki, T., Takai, Y., and Takenawa, T. (1998) *Nature* 391, 93–96.
- Rohatgi, R., Ma, L., Miki, H., Lopez, M., Kirchhausen, T., Takenawa, T., and Kirschner, M. W. (1999) *Cell* 97, 221–231.
- Rohatgi, R., Ho, H. Y., and Kirschner, M. W. (2000) *J. Cell Biol.* 150, 1299–1310.
- Englander, S. W., and Kallenbach, N. R. (1984) *Q. Rev. Biophys.* 16, 521–655.
- Clarke, J., and Itzhaki, L. S. (1998) *Curr. Opin. Struct. Biol.* 8, 122–128.
- Englander, S. W. (2000) *Annu. Rev. Biophys. Biomol. Struct.* 29, 213–238.
- Bai, Y., Milne, J. S., Mayne, L., and Englander, W. (1993) *Proteins: Struct., Funct., Genet.* 17, 75–86.
- Zhang, Y.-Z., Patterson, Y., and Roder, H. (1995) *Protein Sci.* 4, 804–814.
- Jaravine, V. A., Rathgeb-Szabo, K., and Alexandrescu, A. T. (2000) *Protein Sci.* 9, 290–301.
- Buck, M., Radford, S. E., and Dobson, C. M. (1994) *J. Mol. Biol.* 237, 247–254.
- Rudolph, M., Bayer, P., Abo, A., Kuhlmann, J., Vetter, I., and Wittinghofer, A. (1998) *J. Biol. Chem.* 273, 18067–18076.
- Patterson, Y., Englander, S. W., and Roder, H. (1990) *Science* 246, 755–759.
- Williams, D. C., Benjamin, D. C., Poljak, R. J., and Rule, G. S. (1996) *J. Mol. Biol.* 257, 866–876.
- Kheterpal, I., Zhou, S., Cook, K. D., and Wetzel, R. (2000) *Proc. Natl. Acad. Sci. U.S.A.* 97, 13597–13601.
- Alexandrescu, A. T. (2001) *Annu. Pac. Symp. Biocomput.* 6, 67–78.
- Alexandrescu, A. T., Dames, S. A., and Wilschek, R. (1996) *Protein Sci.* 5, 1942–1946.
- Rudolph, M. G., Linnemann, T., Gruenewald, P., Wittinghofer, A., Vetter, I. R., and Herrmann, C. (2001) *J. Biol. Chem.* 276, 2314–2321.
- Buchwald, G., Hostinova, E., Rudolph, M. G., Kraemer, A., Sickmann, A., Meyer, H. E., Scheffzek, K., and Wittinghofer, A. (2001) *Mol. Cell. Biol.* 21, 5179–5189.
- Catimel, B., Teh, T., Fontes, M. R., Jennings, I. G., Jans, D. A., Howlett, G. J., Nice, E. C., and Kobe, B. (2001) *J. Biol. Chem.* 276, 34189–34198.
- Higgs, H. N., and Pollard, T. D. (2000) *J. Cell Biol.* 150, 1311–1320.
- Prehoda, K. E., Scott, J. A., Dyché Mullins, R., and Lim, W. A. (2000) *Science* 290, 801–806.
- Carlier, M. F., Nioche, P., Broutin-l'Hermite, I., Boujemaa, R., Le Clainche, C., Egile, C., Garbay, C., Ducruix, A., Sansonetti, P., and Pantaloni, D. (2000) *J. Biol. Chem.* 275, 21946–21952.
- Rohatgi, R., Nollau, P., Ho, H. Y., Kirschner, M. W., and Mayer, B. J. (2001) *J. Biol. Chem.* 276, 26448–26452.
- Yang, C., Huang, M., DeBiasio, J., Pring, M., Joyce, M., Miki, H., Takenawa, T., and Zigmond, S. H. (2000) *J. Cell Biol.* 150, 1001–1012.
- Zahn, R., Spitzfaden, C., Ottinger, M., Wuthrich, K., and Pluckthun, A. (1994) *Nature* 368, 261–265.
- Zahn, R., Perrett, S., Stenberg, G., and Fersht, A. R. (1996) *Science* 271, 642–645.
- Coyle, J. E., Texter, F. L., Ashcroft, A. E., Masselos, D., Robinson, C. V., and Radford, S. E. (1999) *Nat. Struct. Biol.* 6, 683–690.
- Huntington, J. A., Read, R. J., and Carrell, R. W. (2000) *Nature* 407, 923–926.
- Lefstin, J. A., and Yamamoto, K. R. (1998) *Nature* 392, 885–888.
- Petersen, J. M., Skalicky, J. J., Donaldson, L. W., McIntosh, L. P., Alber, T., and Graves, B. J. (1995) *Science* 269, 1866–1869.
- Kay, L. E., Keifer, P., and Saarinen, T. (1992) *J. Am. Chem. Soc.* 114, 10663–10665.

BI0157215